J Electroceram (2009) 22:156–162
DOI 10.1007/s10832-008-9440-3

Electromechanical performance of structurally graded monolithic piezoelectric actuator

J. Palosaari · J. Juuti · E. Heinonen · V.-P. Moilanen · H. Jantunen

Received: 15 March 2007 / Accepted: 6 February 2008 / Published online: 2 March 2008
© Springer Science + Business Media, LLC 2008

Abstract In this paper, the effect of structural gradients in monolithic piezoelectric actuators is investigated. Different cross-section profiles were micro-machined with a laser into commercial PZT 5H bulk discs with thicknesses of 375 μm and 500 μm (∅ 25 mm). Profiles and curvatures of the actuators were measured which showed both concave and convex structures, thus indicating pre-stress of the actuators. After poling, the distribution of out-of-plane displacement was scanned by a fibre-optic laser vibrometer. Maximum displacements of ~6.3 μm and ~24.8 μm were obtained from a freely moving and clamped ~375 μm thick actuator, respectively, in a ±0.5 V/μm electric field at 10 Hz frequency without load. Furthermore, deflection in the centre of the actuators was measured up to 184 mN load using the same electric field and frequency. Bending of the bulk actuators without any additional layer was a consequence of the gradient in poling and driving electric field via thickness variation of the material. Hence, different regions produced strain distribution and bending in a similar fashion to other benders. Actuators with the highest arch height exhibited the highest displacement and load bearing capabilities derived from the increased area moment of inertia and enhanced piezoelectric response due to pre-stress. The results show that the monolithic bending actuators can be realised by simple structural designing of the actuator. Such structural gradients can be one reason contributing to the higher displacement of RAINBOW actuators compared to other pre-stressed actuators. In a further development, the structural gradients can be utilized in high displacement pre-stressed actuators and in miniaturized monolithic piezoelectric devices.

Keywords Piezoelectric · Gradient · Actuator · Monolithic

J. Palosaari · J. Juuti (✉) · E. Heinonen · V.-P. Moilanen · H. Jantunen
Microelectronics and Materials Physics Laboratories,
EMPART Research Group of Infotech Oulu, University of Oulu,
P.O. Box 4500, Oulu 90014, Finland
e-mail: Jari.Juuti@ee.oulu.fi

J. Palosaari
e-mail: Jaakko.Palosaari@ee.oulu.fi

1 Introduction

Considerable research has been carried out over several decades into materials, structures and devices for electromechanical applications. Well-known piezoelectric materials, like PZT, offer attractive properties such as low energy consumption, quick response, high field-induced stresses and compact size. In order to extend the feasibility of these materials various actuator schemes have been developed to meet different application specifications. One of the schemes is the development of piezoelectric actuators with functional gradients where gradually changing material, stress, composition or porosity have been tailored to modify field-induced stresses, performance, lifetime and reliability [1–6]. In pre-stressed bending actuators, for example, tensile stress varies along the thickness creating a gradient in the piezoelectric d_{31} coefficient and resulting in enhanced displacement capabilities [2, 4, 7]. Among the piezoelectric actuators, the RAINBOW actuator exhibits one of the largest displacement capabilities or effective piezoelectric d_{31} coefficients [8–10]. Contributing factors for the improved performance are suggested to be the mass-loading effect, reduced elastic stiffness, enhanced phase transition and enhanced domain reorientation due to a larger tensile stress compared to corresponding pre-stressed benders [4, 10]. In addition, RAINBOW has a unique

structure due to the reduction process at high temperature creating a non-uniform thickness of the piezoelectric and reduced layer [11–13]. In the earlier analysis only constant thickness for the reduced layer has been used and the effect of the non-uniform actuator geometry in displacement capabilities has not been reported.

In this paper, monolithic piezoelectric bending actuators without any additional layers were manufactured by laser machining and their electromechanical behaviour was characterised. Bending of the actuators is achieved via a structural gradient, similar to RAINBOW, thus creating non-uniform electric and strain fields and an internal bending moment for the piezoelectric material. The effect of the cross-section profile and pre-stress on displacement capabilities is analysed and compared to other pre-stressed actuators.

2 Experiments

Commercial PZT 5H discs (Morgan Electro Ceramics, ∅ 25 mm, thicknesses of 375 μm and 500 μm) without electrodes were micro-machined with a Nd:YVO_4 laser system (Siemens Microbeam 3200, Siemens AG, Germany) to create structures with two different profiles in cross-section, as shown in Fig. 1. The laser machined steps were designed to produce cross-sections with linearly and exponentially increasing thickness towards the edge of the actuators for both sample thicknesses previously used in RAINBOW and THUNDER actuators [10]. The exponential profile was copied from the cross-section of the RAINBOW actuators according to previous experiments [11, 13]. After micro-machining the thinnest part of the actuators was 64% and 46% of the total thickness of 375 μm and 500 μm, respectively. The centre thickness was designed to be slightly less than in the optimal RAINBOW actuators (thickness ratio 25–55%) in order to emphasize the gradient in the electric field [4, 10, 14].

The profile and curvature of the actuators was measured with a DEKTAK3ST Surface Profiler (Veeco, USA). After measurement, electrodes were sprayed on the actuator surfaces using conductive silver paint (Electrolube, UK) with low mechanical strength to avoid the constraining effect of the fired electrodes with its associated additional influence on the bending [15]. The coercive electric field was measured by Radiant RTV6000HVS system (Radiant Technologies, USA) and poling of the actuators was carried out in a 3.0 V/μm electric field in silicone oil at room temperature for 30 minutes. The electric field was determined according to the thinnest region, i.e. the centre area, of the actuators. After a 24 h period had elapsed from the poling, actuators were aged for 10^5 cycles in a ±0.25 V/μm electric field at 100 Hz frequency. Displacement distribution of the structured surface (Fig. 1) along the centreline of the free and clamped actuators was measured in a ±0.5 V/μm electric field at 10 Hz frequency using a fibre-optic laser vibrometer OFV-5000 (Polytec GmbH, Germany) and XY-table [16, 17]. Additionally, displacement at the centre of the free gradient actuators was measured from ±0.1 V/μm to ±0.5 V/μm electric fields at 10 Hz frequency under applied weights up to 18.8 g. Stiffness of a PZT 5H bulk disc and micro-machined actuators was measured utilising the measurement system presented by Juuti et al. [15]. The actuators were placed freely on an alumina ring in order to allow larger bending of the samples. Forces were applied at the middle of the smooth surface and deflection was detected from the bottom surface by an interferometer. In addition, the piezoelectric d_{31} coefficient was determined with ±0.1 to ±0.5 V/μm electric fields at 10 Hz frequency by measuring the transversal displacement of the rectangular PZT 5H bulk sample clamped at one end.

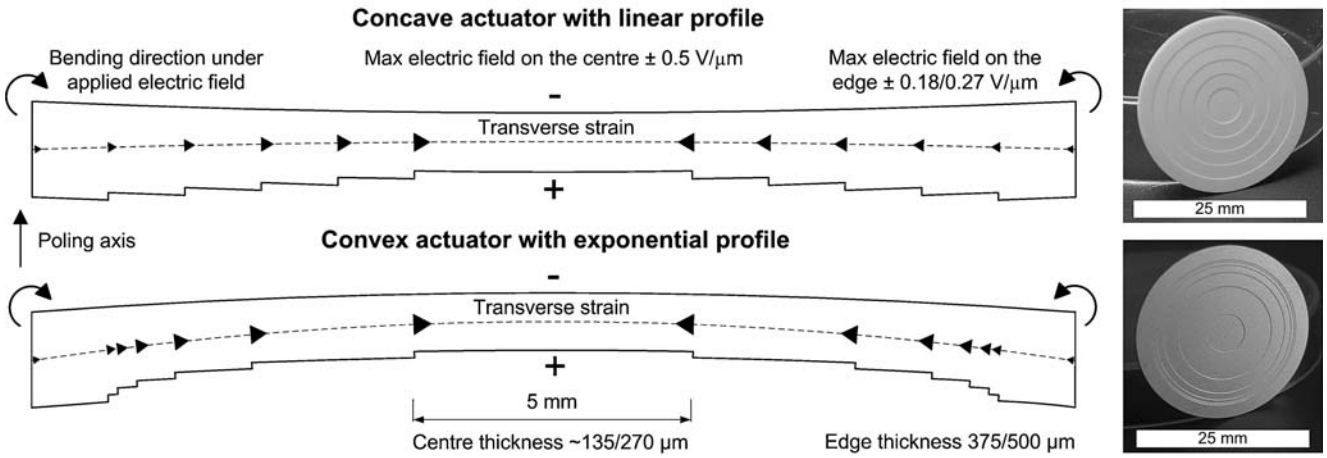

Fig. 1 Schematic profiles and pictures of the actuators with (**a**) linearly and (**b**) exponentially increasing thickness towards the edges

3 Results and discussion

Schematics of the actuator profiles and their pictures and operation principles are shown in Fig. 1, where larger arrows on the centreline of the actuators indicate greater transverse strain via piezoelectric coefficient d_{31} as the electric field increases from edge to centre due to the thinner piezoelectric layers. Actuators bend downwards in an electric field parallel to poling as a consequence of the gradients in polarisation and driving electric field, hence producing a strain difference between outer and inner regions and actuation similar, for example, to a unimorph, RAINBOW or polarisation graded ferroelectric plate [2, 18]. Actuators exhibited initial curvature after manufacture indicating a pre-stress as a consequence of the laser micro-machining. The arch height and shape of each actuator before and after poling is shown in Table 1. The convex structure is similarly domed as in RAINBOW actuators i.e. upwards in Fig. 1 while the concave structure is curved downwards. In such cases, tensile stress is present on the top surface, possibly enhancing the gradient of the piezoelectric d_{31} coefficient in addition to the gradient produced by poling [4]. In contrast, the top surface of the concave structure is expected to be subjected to a compressive stresses. Arch height of the actuators was decreased after poling except in the case of the one 500 μm thick exponential convex structure (Table 1). The actuators minimise their internal stresses in a poling field by changing their shape, thus the structure flattens in general by a polarisation induced self-strain opposite to the pre-stress. However, the curvature and shape after poling depends on the actuator geometry, shape, residual stresses, poling induced stresses and stress relaxation mechanisms which may also lead to increased curvature. For example, an initially flat polarisation graded ferroelectric plate is expected to be domed as a consequence of self-strain through poling [18].

Under the poling condition for example a 500 μm thick actuator with a linear profile exhibited coercive electric field of ±1.6 V/μm. Accordingly the driving fields were selected well below typical field limits to avoid de-poling (±1/3 of the coercive field) [19]. The coercive field result is comparable to values obtained from a closely corresponding pre-stressed PRESTO actuator ($E_{cPRESTO}$ =+1.6/−1.8 V/μm) and higher than showed by a bulk actuator (E_{cbulk}=+ 1.2/−1.2 V/μm) as a consequence of the gradient in the electric field and slight pre-stress in the structure [20]. More detailed analysis will be reported elsewhere.

Displacement distributions along the centreline of the free actuators in a ±0.5 V/μm electric field are shown in Fig. 2. The actuators exhibit 1.5–6.3 μm axial displacement by bending. Comparison of structures shows that pre-stress producing the highest arch height (Table 1) significantly enhances displacement capabilities, as can be expected regarding earlier results obtained with RAINBOW actuators [2, 4]. In the 375 μm thick concave actuators with nearly the same curvature [Fig. 2(a)] larger displacement is obtained with the linear profile. This is a consequence of an evenly distributed and slightly greater amount of material (Fig. 1, below the thinnest region) that forces the structure to bend via the greater electric field and strain differences in adjacent regions compared to the case of an exponential profile. The particular displacement shown at the edges of the actuators (Fig. 2) is a consequence of the structure having a node point on the edge of the first laser-machined layer.

The largest displacements were also obtained by convex structures when actuators were clamped at the edges (Fig. 3) by pressing both surfaces with a mechanical setup and rubber ring (inner diameter 24 mm). In such cases the displacement of the actuators was significantly improved, partially because movement of the edges was not allowed in the same way as without clamping in Fig. 2. Additionally, clamping constricted the transverse strain of the actuator, especially at the lower part under the thinnest region in Fig. 1, enabling a larger difference in strain and greater bending moment, thus producing a larger axial displacement. It should also be noted that the order of the displacement generation remained the same between freely moving and clamped actuators, thus a 375 μm thick exponential convex actuator exhibited the highest displacement in both the free and clamped conditions.

The gradient actuators show opposite characteristics between free and clamped conditions to those obtained by Mulling et al. for THUNDER actuators where the actuator displacement was the greatest in the unconstrained end

Table 1 Thickness, shape and arch height of the actuators.

Thickness	375 μm	375 μm	375 μm	500 μm	500 μm	500 μm
Profile and shape	Linear, concave	Exponential, convex	Exponential, concave	Linear, concave	Exponential, convex	Exponential, convex
Initial arch height [μm]	50	130	65	63	40	90
Arch height after poling [μm]	35	125	30	30	20	110

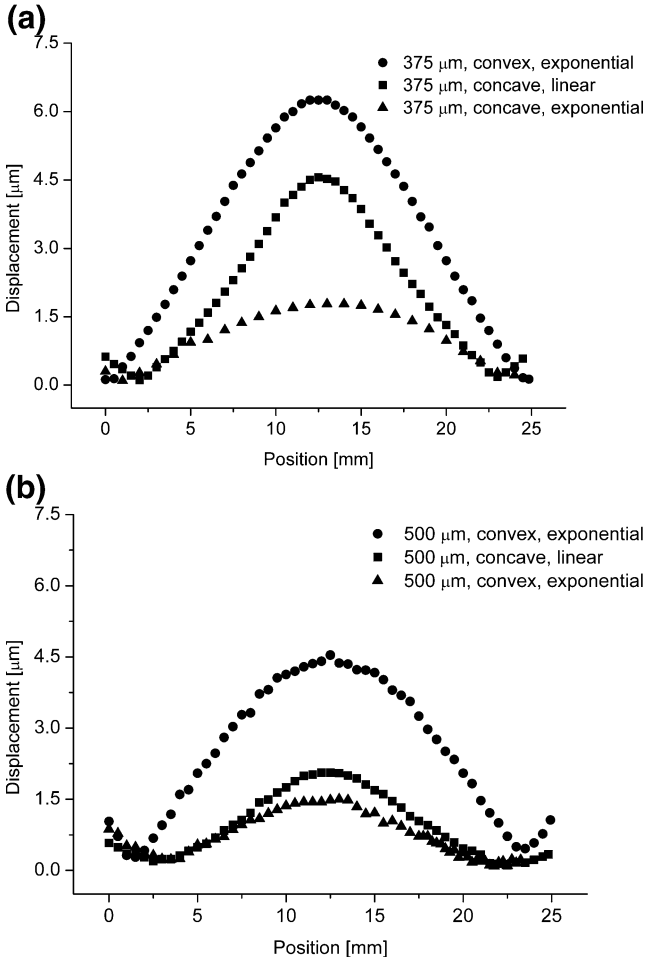

Fig. 2 Displacement distribution along the centreline of the (**a**) 375 μm and (**b**) 500 μm thick free actuators in ±0.5 V/μm electric field and without load

conditions [21]. The reason is believed to be in the actuator structures because the gradient actuators are designed to be utilised with solid clamping, thus having only a slight restraining of transverse strain initially. In the THUNDER actuators the transverse strain is already strongly restrained by passive metal layers in order to obtain the maximum bending moment in the free condition. In the case where rotation and translation of the PZT 5A THUNDER actuator (ceramic part $38.1\times12.7\times0.2$ mm^3) was blocked it exhibited approximately 40 μm displacement whereas in free conditions it obtained approximately 230 μm displacement with 1.08 V/μm electric field [21]. The clamped displacement of the gradient actuator is quite comparable with the blocked THUNDER considering the differences in material and size yet the displacement of the gradient actuators may be increased by improved clamping and optimised profile.

Displacement at the centre of the gradient actuators and the d_{31} coefficient of the bulk actuator as a function of driving electric field are shown in Fig. 4. The bulk actuator exhibits nearly linear behaviour of its piezoelectric coefficient d_{31} which should produce a slightly non-linear displacement increase as a function of electric field, whereas gradient actuators generate an exponential increase [22]. Such behaviour has also been observed for other bending type actuators such as unimorph, bimorph, LIPCA and RAINBOW in quasistatic and resonance conditions. The behaviour is related to the increasing elastic compliance of the ceramic due to elastic non-linearity as a function of electric field. [22, 23] Thus, a decreased Young's modulus accumulates greater deflection due to lower stiffness under increasing electric field. Furthermore, in both the thicknesses non-linearity seems to increase as a function of arch height thus indicating that a higher level of pre-stress contributes to the behaviour. Increasing non-linearity as a function of pre-stress has also been obtained for RAINBOW actuators by Schwartz et al. with electric fields below 0.16 V/μm in quasistatic conditions. This is expected to be a result of enhanced extrinsic contributions (domain configuration and domain wall motion) at higher electric fields and stresses while intrinsic piezoelectric contributions dominate at low electric fields. [4] Moreover,

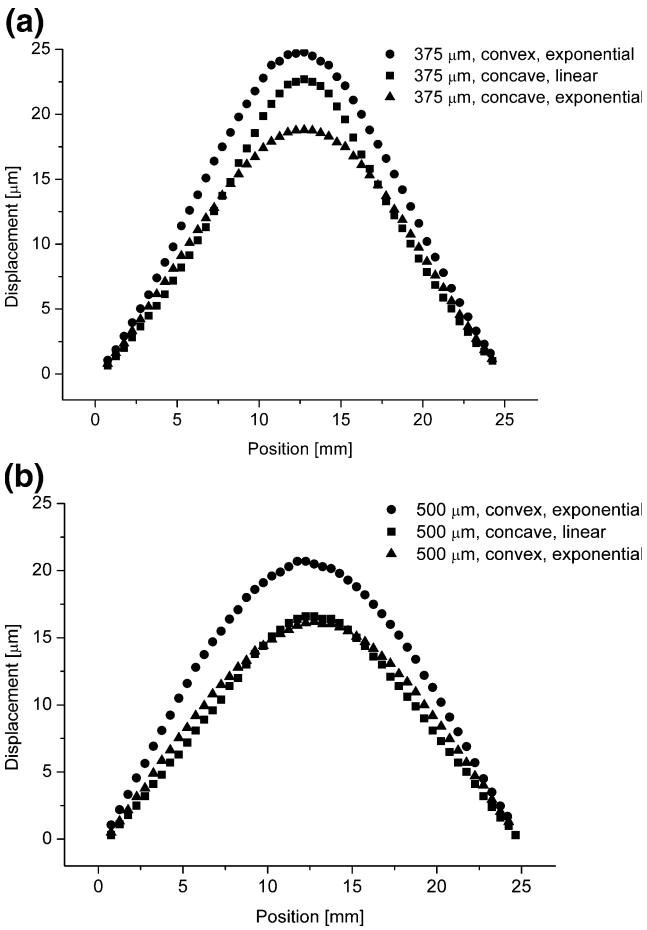

Fig. 3 Displacement distribution along the centreline of the (**a**) 375 μm and (**b**) 500 μm thick actuators clamped at the edges in a ±0.5 V/μm electric field and without load

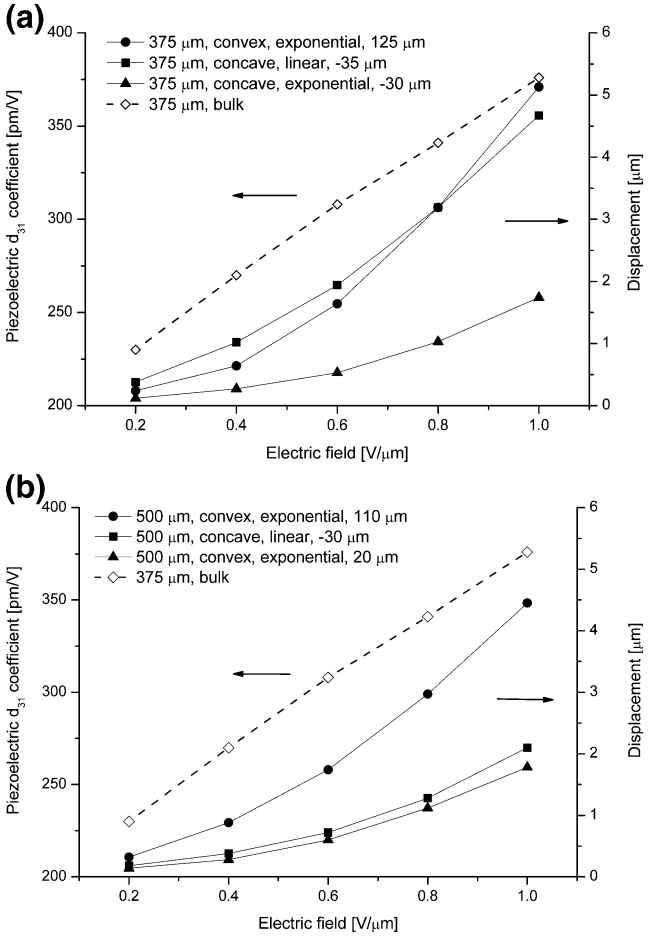

Fig. 4 Centre displacement of free gradient actuators with thickness of (**a**) 375 μm and (**b**) 500 μm and d_{31} coefficient of bulk actuator as a function of electric field

displacements of the linear profiles are increasing more rapidly than their close counterparts with exponential profiles, probably due to the higher difference in electric field mentioned earlier.

Results of displacement measurements under load are shown in Fig. 5 as normalised values. Actuators with a convex structure exhibited significantly greater load bearing capability due to pre-stress i.e. increased geometric moment of inertia and improved displacement capabilities. The enhanced displacement capabilities are expected to be a consequence of tensile stress on the top of the convex surface creating an additional gradient of the piezoelectric d_{31} coefficient. The same situation exists in RAINBOW actuators as a result of the reduction process. For example, a PZT 5H RAINBOW actuator (∅ 25.4 mm, piezoelectric ceramic and metal thicknesses 381 μm and 127 μm, respectively) was reported to obtain ~17% higher displacement, i.e. 10 μm difference, than a corresponding THUNDER actuator in a ±0.5 V/μm electric field, without load and at 1 Hz frequency [10]. One contributing factor to the difference could be the non-uniform poling and driving electric field in the RAINBOW while the thickness of the piezoelectric layer in the THUNDER actuator is constant. Convex actuators generated 4.5–20.7 μm displacement depending on clamping [Figs. 2(b) and 3(b), thickness of 500 μm and 270 μm on the perimeter and centre, respectively], which would be a significant part of the difference between the actuators. However, it should be kept in mind that the magnitude of the effect may change via the applied passive layer and for more detailed analysis a cross-section profile of the RAINBOW would be required.

Displacement differences between exponential convex and concave structures under the highest load were ~63% for 375 μm actuators. The corresponding value for 500 μm thick exponential actuators was ~180% with dome height difference of 90 μm (Table 1). In this case the effect of the non-uniform electric field remains basically the same and the result clearly shows the large impact of the pre-stress.

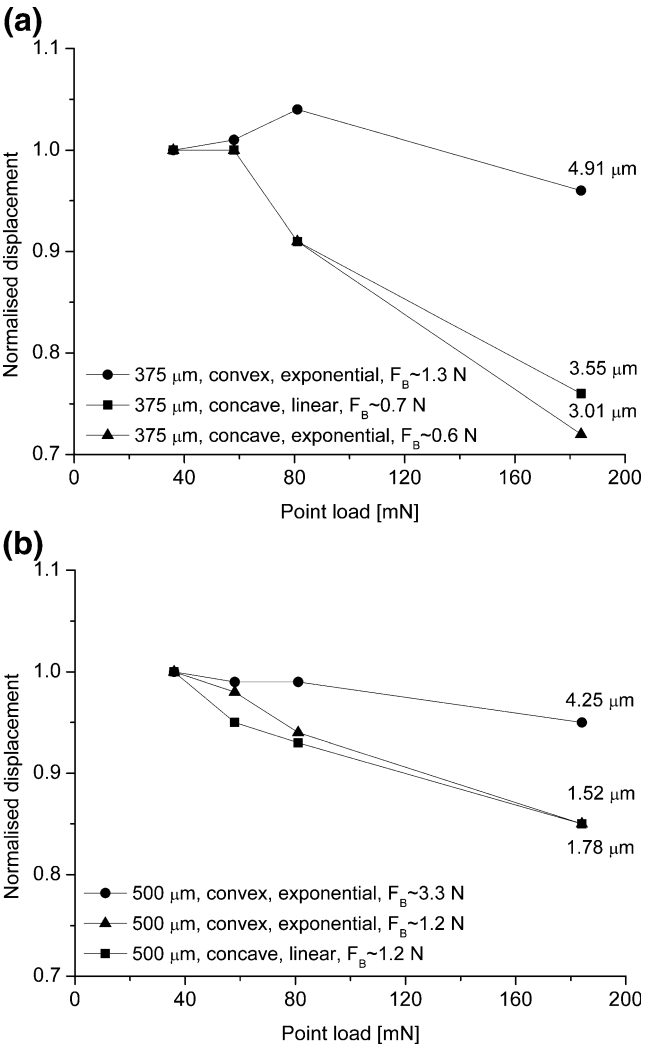

Fig. 5 Normalised displacement of free gradient actuators with thickness of (**a**) 375 μm and (**b**) 500 μm in a ±0.5 V/μm electric field as a function of load

Larger difference in 500 μm thick actuators is expected to be a consequence of larger pre-stress derived from the thicker actuator and curvature. Estimated blocking forces (F_B) of 375 μm and 500 μm thick actuators were 0.6–1.3 N and 1.2–3.3 N, respectively, based on linear approximations from the last two values in Fig. 5. The values are modest compared to values of RAINBOW, THUNDER or PRESTO, but can be significantly improved by increased pre-stress, addition of passive material or proper clamping [15].

In general, the effect of thickness on load bearing and displacement capability between 375 μm and 500 μm thick actuators showed the expected result i.e. thinner actuators being weaker but generating higher displacements. The linear profile exhibited slightly higher displacements and about equal blocking forces compared to its close counterpart with an exponential profile (Fig. 5). However, the possible influence of different curvatures should be recognised. In order to identify the overall effect of the actuator geometry on the stiffness, the area moment of inertia was calculated for the cross-sections of bulk actuators, gradient actuators based on the profile measurements and corresponding actuators without curvature (Fig. 6). Moreover, the measured stiffness of the gradient actuators and calculated stiffness of the bulk actuators derived from measured value are shown in the figure. As shown in Fig. 6, convex shaped gradient actuators exhibited a significantly higher area moment of inertia compared to their flat counterpart, i.e. without curvature, while concave (negative arch height values in Fig. 6) structures obtained slightly decreased values. The difference (upper percentages in Fig. 6) is even greater compared to the values of the uniform bulk actuators with the same average thickness. A similar trend would be expected for the stiffness or flexural rigidity which is a product of the area moment of inertia, Young's modulus and boundary conditions (same in each

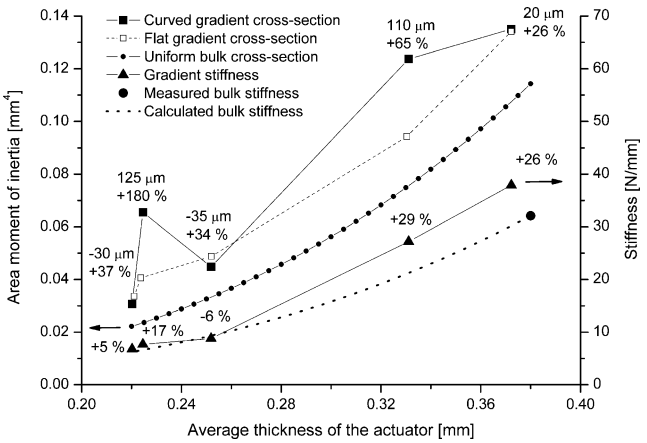

Fig. 6 Area moment of inertia, arch height and measured and calculated stiffness of the gradient and bulk actuators as a function of average thickness

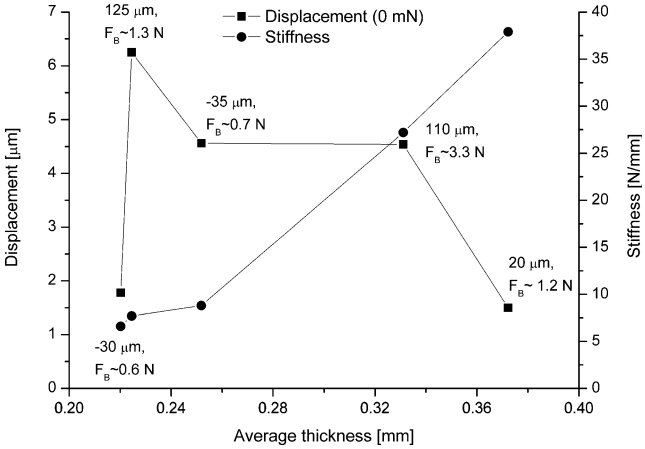

Fig. 7 Stiffness and free displacement of the gradient actuators as a function of average thickness

measurement). In spite of this, only slight changes from −6% to 29% can be seen in stiffness. The result can be influenced by compositional changes in the laser machined surface and its height variation which were averaged in the calculation. However, the main reason for the result is expected to be non-linear stress-strain behaviour of the piezoelectric ceramic i.e. altered Young's modulus under pre-stress by manufacturing and poling. Tensile stress perpendicular to the poling field can decrease Young's modulus down to ~49% at ~48 MPa from initial low stress values depending on composition, stress level and electrical conditions [14, 24–26]. It should be pointed out that another surface of the curved structure is under compressive stress and therefore also susceptible to altered elastic properties. For the concave structures it is expected that tensile stress is present on the lower surfaces while the upper surface is under compression.

Stiffness and displacement of the gradient actuators as a function of average thickness are shown in the Fig. 7 indicating also the arch height and estimated blocking force. Fundamentally, displacement of the piezoactuator decreases as the stiffness increases. Roughly the same trend can be seen here which, however, is disturbed by the influence of different profiles and levels of the pre-stress. Peculiar characteristics are obtained with the 500 μm thick convex exponential actuator (height 110 μm) retaining the displacement capabilities while the stiffness and blocking force are significantly increased. The reason is expected to be a proper combination of pre-stress enhancing the piezoelectric d_{31} coefficient and stiffness via increased area moment of inertia.

Furthermore, discrepancies between stiffness and estimated blocking forces were observed as the stiffest actuator did not attain the highest blocking force. It likely that the used linear extrapolation is too simple to estimate blocking force reliably as the actuators will experience various levels

of stresses under increased loading which in turn will alter the Young's modulus and deflection under load. However, the blocking force is also affected by the level of displacement which increases as a function of the d_{31} coefficient via tensile pre-stress [4]. For example, blocking force differences of two last values in Fig. 7 can be mainly explained by displacement differences because the actuator with a height of 110 μm exhibits ~3 times higher displacement than the actuator with a height of 20 μm.

The load bearing capability of the actuators was dictated by pre-stress resulting in increased stiffness and displacement capability via changed area moment of inertia and enhanced extrinsic contributions. Additionally, the linear profile in the 375 μm thick actuator produced slightly higher stiffness as a consequence of the greater area moment of inertia. In the 500 μm thick actuators, substantial differences between profiles were not observed. All actuators exhibit remarkably larger displacements than would be achieved with a simple bulk actuator of the same size. Thus structural gradients are one additional way to produce bending actuators and improve their displacement capabilities. Furthermore, proper pre-stress and clamping by mechanical construction or passive material (as in RAINBOW actuators) can significantly improve the obtained displacement capabilities that can be utilised in e.g. embedded actuator structures.

4 Conclusions

Structurally graded piezoelectric bulk actuators were introduced and the displacement capabilities of different cross-section profiles were tested. The results show that by utilising the electric field gradient, bending actuators can be realised from bulk samples without any additional layer. The same effect can be present in RAINBOW actuators, thus partially explaining their higher displacement capabilities compared to other corresponding actuators. Additionally, the results showed the effect of the profile and the significant influence of the pre-stress on the displacement and load bearing capabilities. In order to improve displacement capabilities of the piezoelectric actuators even further it is also important to utilise the effects of the geometry. In further development, the structural gradients can be utilised in high displacement pre-stressed actuators and in miniaturized devices with minimal influence of thermally derived stresses due to the monolithic structure.

Acknowledgement The work was performed under the Hi-Piezo project (number 124011) funded by the Academy of Finland. Authors J. Palosaari and E. Heinonen gratefully acknowledge the financial support of the Jenny and Antti Wihuri foundation and Infotech Oulu graduate school.

References

1. A. Hall, M. Allahverdi, E. K. Akdogan, A. Safari, J. Eur. Ceram. Soc **25**, 2991 (2005)
2. G. Li, E. Furman, G.H. Haertling, J. Am. Ceram. Soc. **80**(6), 1382 (1997)
3. X. Li, J.S. Vartuli, D.L. Milius, I.A. Aksay, W.Y. Shih, W.-H. Shih, J. Am. Ceram. Soc. **84**(5), 996 (2001)
4. R. W. Schwartz, L. E. Cross, Q. M. Wang, J. Am. Ceram. Soc. **84** (11), 2563 (2001)
5. K. Takagi, J.-F. Li, S. Yokoyama, R. Watanabe, J. Eur. Ceram. Soc. **23**, 1577 (2003)
6. M. Taya, A. A. Almajid, M. Dunn, H. Takahashi, Sens. Actuators A Phys. **107**, 248 (2003)
7. X. Li, W. Y. Shih, J. S. Vartuli, D. L. Milius, I. A. Aksay, W.-H. Shih, J. Am. Ceram. Soc. **85**(4), 844 (2002)
8. J Juuti, ACTA Universitatis Ouluensis C 235, (2006) Available at http://herkules.oulu.fi/isbn9514279891/
9. A. J. Moskalik, D. Brei, Smart Mater. Struct. **8**, 531 (1999)
10. S. A. Wise, Sens. Actuators A Phys. **69**, 33 (1998)
11. J. Juuti, E. Heinonen, V.-P. Moilanen, S. Leppävuori, J. Eur. Ceram. Soc. **24**, 1901 (2004)
12. Q.-M. Wang, L. E. Cross, Mater. Chem. Phys. **58**, 20 (1999)
13. E. Heinonen, J. Juuti, S. Leppävuori, J. Eur. Ceram. Soc. **25**, 2467 (2005)
14. Q.-M. Wang, L. E. Cross, J. Am. Ceram. Soc. **82**(1), 103 (1999)
15. J. Juuti, H. Jantunen, V.-P. Moilanen, S. Leppävuori, IEEE Trans. Ultrason. Ferroelectr. Freq. Control **53**(5), 838 (2006)
16. Z. Huang, G. Leighton, R. Wright, F. Duval, H. C. Chung, P. Kirby, R. W. Whatmore, Sens. Actuators A Phys. **135**(2), 660 (2006)
17. K. Yao, F. E. H. Tay, IEEE Trans. Ultrason. Ferroelectr. Freq. Control **50**(2), 113 (2003)
18. S. Zhong, Z.-G. Ban, S. P. Alpay, J. V. Mantese, Appl. Phys. Lett. **89**, 142913 (2006)
19. J. Hughes, P. G. Bednarchik, in *Proceedings of the 12th IEEE International Symposium on Applied Ferroelectrics,* Honolulu, Hawaii, **1**, 41 (Jul 21–Aug 2 2000)
20. J. Juuti, H. Jantunen, V.-P. Moilanen, S. Leppävuori, J. Electroceram. Soc. **15**, 57 (2005)
21. J. Mulling, T. Usher, B. Dessent, J. Palmer, P. Franzon, E. Grant, A. Kingon, Sens. Actuators A Phys. **94**, 19 (2001)
22. Q.-M. Wang, Q. Zhang, B. Xu, R. Liu, L. E. Cross, J. Appl. Phys. **86**(6), 3352 (1999)
23. S.-C. Woo, K. H. Park, N. S. Goo, Sens. Actuators A Phys. **137**, 110 (2007)
24. T. Fett, D. Munz, G. Thun, J. Mater. Sci. Lett. **18**, 1899 (1999)
25. O. Guillon, F. Thiebaud, P. Delobelle, D. Perreux, Mater. Lett. **58**, 986 (2004)
26. T. Tanimoto, K. Yamamoto, T. Morii, in *Proceedings of the 9th IEEE International Symposium on. Applied Ferroelectrics,* Pennsylvania, USA **394** (Aug 7–10 1994)